Numerical Simulation of the SLAC X–100 Klystron Using RKTW2D*

Robert D. Ryne
Lawrence Livermore National Laboratory, Livermore, CA 94550

Arnold E. Vlieks
Stanford Linear Accelerator Center, Stanford, CA 94309

Abstract

We have performed numerical simulations of the X–100 klystron being developed at Stanford Linear Accelerator Center. The X–100 is being developed as a possible source for the next generation of linear collider, and will be required to produce ≈100 MW of power for a duration of ≈800 ns. Our simulations were performed using the simulation programs RKTW1D and RKTW2D, developed at Lawrence Livermore National Laboratory. The codes were used to investigate the operation of the klystron over a wide range of operating conditions. We will present comparisons of the simulation results with experimental results.

I. INTRODUCTION

The X-100 klystron, under development at the Stanford Linear Accelerator Center, is being developed as a possible power source for the next generation of linear collider.[1] The X-100 is a 440 keV, 510 amp klystron that operates at 11.4 GHz. It will be required to produce ≈100 MW of power for a duration of ≈800 ns; binary pulse compression will result in a 500 MW, 100 ns rf pulse. So far, the klystron has produced 72 MW of power.

We have performed 1D and 2D simulations of the X-100 with the simulation programs RKTW1D and RKTW2D. Our simulations, based on a simplified model of the output cavity, predict that the klystron will produce 72 MW of power at 440 keV and 450 amps. Below we discuss the structure of the klystron codes and the details of our simulations.

II. KLYSTRON SIMULATION PROGRAMS

RKTW1D and RKTW2D are computer programs that simulate the operation of relativistic klystrons. Both codes are time-dependent, and both assume that the fields in the problem are cylindrically symmetric. RKTW1D is a fast running, 1–dimensional code, while RKTW2D is a slower 2–dimensional code that more accurately models the physical system under consideration. The codes follow a train of RF bunches, one at a time, through a klystron. The codes have the following features:

1. self-consistent beam-cavity interaction
2. self-consistent space charge
3. time-dependent cavity excitation modelled using circuit equations
4. treatment of standing wave (SW) cavities and traveling wave (TW) structures

Prior to executing the klystron codes, one must run SUPERFISH to calculate the eigenmodes of the cavities in the problem.[2] (It is assumed that a single mode is dominant in each of the cavities.) Furthermore, one must run a preprocessor to interpolate the SUPERFISH data onto a uniform rectangular mesh that can be used by the klystron codes. If there are TW structures in the problem, the TW fields are calculated by appropriate superposition of the standing wave SUPERFISH results.

The klystron codes have the ability to read in a particle distribution generated by the electron gun code EGUN.[3] The codes can also read in magnetic field data produced by the magnet design code POISSON.[2]

The basic equations used by the klystron codes are the single particle equations of motion and the circuit equations governing cavity excitation. The single particle equations of motion are the Lorentz force equations using the longitudinal coordinate, z, as the independent variable:

$$\begin{aligned}
\frac{dx}{dz} &= v_x/v_z, \\
\frac{dy}{dz} &= v_y/v_z, \\
\frac{d\psi}{dz} &= \omega/v_z, \\
\frac{dv_x}{dz} &= \frac{q}{\gamma m}\left(\vec{E}+\vec{v}\times\vec{B}\right)_x - \frac{\beta_x}{c}\vec{v}\cdot\vec{E}, \\
\frac{dv_y}{dz} &= \frac{q}{\gamma m}\left(\vec{E}+\vec{v}\times\vec{B}\right)_y - \frac{\beta_y}{c}\vec{v}\cdot\vec{E}, \\
\frac{d\gamma}{dz} &= \frac{q}{mc^2 v_z}\vec{v}\cdot\vec{E},
\end{aligned} \tag{1}$$

where $\psi = \omega t$. (Transverse motion is neglected in the 1–d code.) Beam induced cavity excitation is based on a circuit equation for SW cavities or based on coupled circuit equations for TW structures. Consider the analysis of a TW structure. Assuming a single cavity mode is dominant, let the electric field in the n^{th} cell of the structure be given by

$$\vec{E}_n(\vec{r},t) = f_n\,\vec{\mathcal{E}}_n(\vec{r})\,e^{-i\omega t}, \tag{2}$$

where $\mathcal{E}_n$ denotes an eigenmode with eigenfrequency ω_n. Also, let ω denote the drive frequency of the klystron.

* Work supported by the US Department of Energy contracts W-7405–ENG-48 (LLNL) and DE-AC03–76SF00515 (SLAC)

Then it is possible to show that the excitations f_n are governed by the following coupled equations

$$\ddot{f}_n + \left(\frac{\omega_n}{Q_n} - 2i\omega\right)\dot{f}_n + \left(\omega_n^2 - \omega^2 - \frac{i\omega\omega_n}{Q_n}\right)f_n \\ -(K_n^{n-1}f_{n-1} + K_n^{n+1}f_{n+1}) = \frac{i\omega}{\epsilon_o}\int dV_n\, \vec{\mathcal{E}}_n^* \cdot \vec{J}_1, \tag{3}$$

where Q_n denotes the quality factor of the n^{th} cell, K_n^{n-1} and K_n^{n+1} denote coupling of the cell n to cell $n-1$ and cell $n+1$, respectively, and $\vec{J}_1$ denotes the RF current associated with the beam. (For a SW cavity, the above set of coupled equations is replaced by a single equation with n=1 and with the coupling constants set equal to zero.)

III. SIMULATION RESULTS

The X-100 klystron consists of an input cavity, three gain cavities, and an output cavity. The klystron operates at 440 keV, 510 amp and at a frequency of 11.4 GHz. The experimental results that we will discuss are based on a double gap, standing wave output cavity. The double gap cavity exhibits lower peak fields than a conventional single gap cavity. However, the double gap cavity does not have cylindrical symmetry, so it cannot be modeled realistically with our klystron codes. Instead, our simulation results are based on a single gap output cavity. Two other important features of our simulation are the following: (1) The beam distribution used by RKTW2D was produced by the electron gun program EGUN; (2) the magnetic field profile used by RKTW2D was produced using POISSON.

Our main results are summarized in Figure 1. Figure 1 shows the klystron output power as a function of beam energy (using a fixed magnetic field profile). The crosses denote experimental results; the dashed line denoted 1d simulation results and the solid line denotes 2d results. At low power, RKTW1D and RKTW2D give nearly identical results, and both are comparable with experimental values. At high power, both codes predict power levels that are greater than or equal to the experimental results, with the 2d code showing better agreement than the 1d code. The main difference between the 2d results and the experimental results is that the 2d results show a peak in output power near 433 kV; however, as we will show below, this is do to current loss in the 440 kV calculation and not do to saturation of the klystron.

The time-dependent nature of our simulations is shown in Figure 2. This figure shows the power output as as a functions of time for the 440 kV case with a 75 W drive. The klystron reaches steady state in less than 20 ns.

Figure 3 shows the RF current as a function of z at 440 kV for three drive powers, 35 W, 50 W and 75 W. The peak rf current with a 75 W drive is 555 amp. A similar plot for the 433 kV case shows that the peak rf current is 615 amp.

Figure 4 shows the DC current as a function of z at 433 kV and 440 kV. In both cases, the EGUN input file has an initial current of 500 amp. RKTW2D predicts that 50 amps of current is spilled at the klystron entrance in the 440 kV case, but only 10 amp is spilled in the 433 kV case. This accounts for why the code predicts more power at 433 kV. The initial beam radius is slightly larger in the 440 kV case. Figure 5 shows the edge radius and the rms radius of the beam for the two cases. The radius of the beam pipe is 4.7 mm.

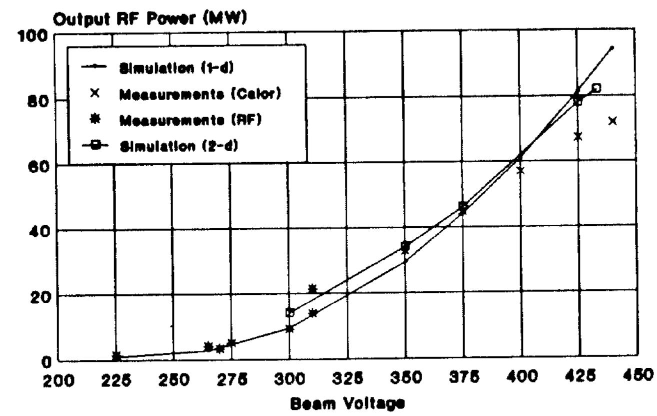

Figure 1 Output power as a function of beam energy: simulation and experiment

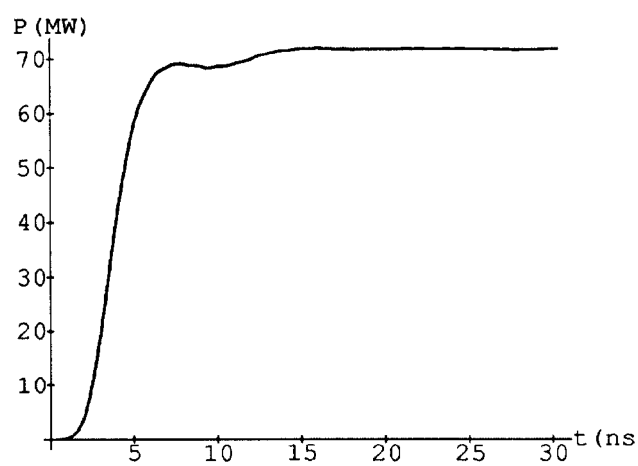

Figure 2 Output power as a function of time (E=440 kV)

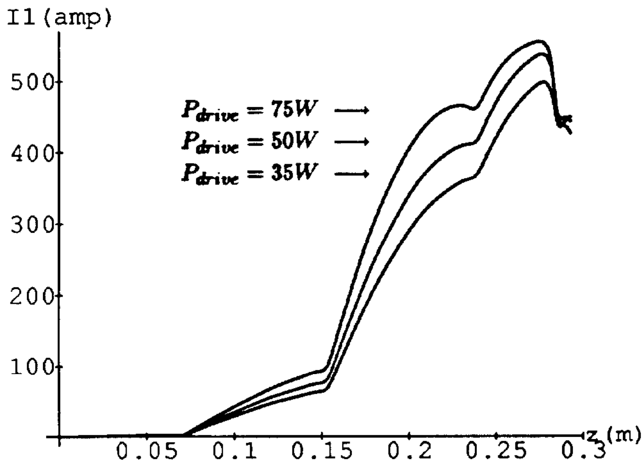

Figure 3 RF current as a function of z (E=440 kV)

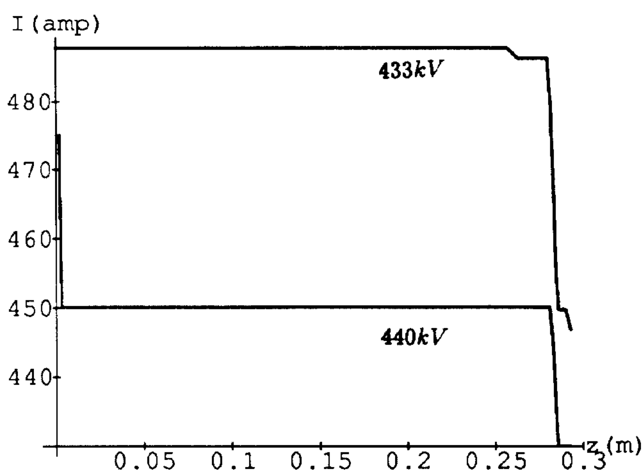

Figure 4 DC current as a function of z

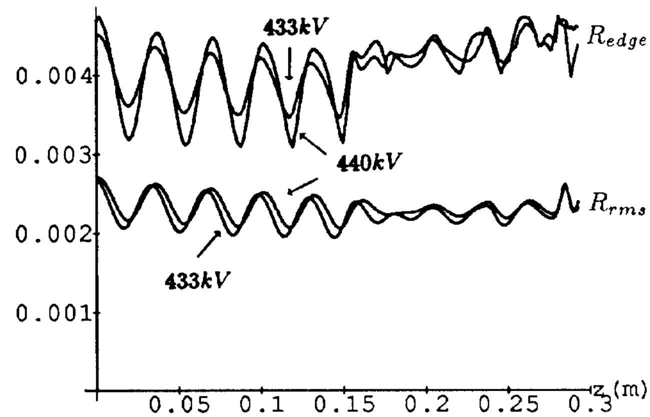

Figure 5 Edge radius and rms radius as a function of z

IV. Summary

We have performed numerical simulations of the X-100 klystron using RKTW1D and RKTW2D. The simulation results are in good agreement with experimental results. The simulation results are sensitive to the initial beam distribution, since the initial beam appears to have a radius approximately equal to the pipe radius. In the future we plan to do simulations of the X-100 with a traveling wave output structure.

V. Acknowledgments

The authors thank E. Wright for performing the EGUN runs that were used to generate the initial beam distributions for the klystron simulations.

VI. References

1. A. E. Vlieks et. al., "100 MW Klystron Development at SLAC," published in this volume.

2.Los Alamos Accelerator Code Group, "Reference Manual for the POISSON/SUPERFISH Group of Codes," LA-UR-87-126 (1987)

3. W. B. Hermannsfeldt, "EGUN — An Electron Optics and Gun Design Program," SLAC Report 331 (October 1988)